RSC Advances

Bottom-up molecular-assembly of Ru(II)polypyridyl complex-based hybrid nanostructures decorated with silver nanoparticles: Effect of Ag nitrate concentration

Journal:	*RSC Advances*
Manuscript ID:	RA-ART-02-2014-001347.R2
Article Type:	Paper
Date Submitted by the Author:	11-Apr-2014
Complete List of Authors:	Narayanasamy, Vilvamani; Delhi University, Chemistry Department Gupta, Tarkeshwar; Delhi University, Chemistry Department Gupta, Rinkoo; South Asian University, Faculty of Life sciences and Biotechnology Awasthi, Satish; Delhi University, Delhi, Chemistry Department

Cite this: DOI: 10.1039/c0xx00000x

www.rsc.org/xxxxxx

ARTICLE TYPE

Bottom-up molecular-assembly of Ru(II)polypyridyl complex-based hybrid nanostructures decorated with silver nanoparticles: Effect of Ag nitrate concentration

Narayanasamy Vilvamani[a], Tarkeshwar Gupta[a], Rinkoo Devi Gupta[b]*, and Satish Kumar Awasthi[a]*

Received (in XXX, XXX) Xth XXXXXXXXX 20XX, Accepted Xth XXXXXXXXX 20XX
DOI: 10.1039/b000000x

Ruthenium functionalized silver nanocomposites (Ag NCs) and hybrid nanotubes (HNTs) were prepared in a one-pot process using tris(4,4'-dicarboxy-2,2'- bipyridyl)ruthenium(II)- sensitizer as reducing and molecular capping reagent involving Ag nitrate as metal precursor. Ag NCs and HNTs were architectured with unique structural features by tuning Ag nitrate concentration while keeping other parameters constant such as temperature, time, and solvent of the reaction by exploiting bottom-up approach. The newly synthesized hybrid materials were well characterized by various electron microscopic methods such as transmission electron microscopy (TEM) and scanning electron microscopy (SEM) and powder X-ray diffraction (PXRD) studies. TEM and SEM studies revealed the morphological features of Ag NCs and HNTs. PXRD study showed the crystallinity of Ag NPs having (111) crystal plane on HNTs. Optical properties have been studied through UV-vis, fluorescence and Raman spectroscopy and showed the formation of Ag NPs decorated hybrid nanostructures with fluorescent properties and enhanced Raman scattering properties. The presence of morphological diversity in Ag nanohybrids formation studied in detail by comparing structural features of capping molecules, Ru (II)-sensitizer and trisodium citrate.

1. Introduction

One dimensional (1-D) inorganic hybrid nanostructures tailored with desirable shape and structure is of great interest in the field of nanoelectronics,[1] nanobioelectronics,[2] energy storage and conversion,[3] photocatalytic,[4] and SERS processes.[5] Among the abundant inorganic nanotube chemistry evolved in the past decade, the incorporation of one-dimensional nanostructures along with zero dimensional nanoparticles into hybrid structures have received much attention in recent years.[6-7] These nanoparticle-loaded HNTs often possess extraordinary structural, electrochemical, electromagnetic, and other properties that are not available to the respective components alone.[8]

Several nanoparticles, prepared from variety of materials including metals, semiconductors and polymers, act as suitable building blocks for complex nanoscaled material architectures.[9-12] Their dimensions, typically several nm to hundred nm, provide unique flexibility in the synthesis of hybrid nanomaterials with desirable morphologies. Examples include controlled aggregation in solution,[13] as well as binding to templates such as macro-molecules,[14] and to solid substrates of planar[15] or curved[16] geometries. For example, Lahav et al. used amine functionalized monolayer on nanoporous alumina as a structure directing template to form gold nanoparticle nanotubes.[17]

The first study on a metal nanoparticle decorated carbon nanotubes reported by Planeix et al. using hydrogen as reducing agent for an organic ruthenium salt in the presence of SWCNTs.[18] Since, such a carbon nanotube incorporated hybrid material synthetic process involves the reduction of metal precursor using sodium borohydride[19] or ethylene glycol as a medium.[20] Alternatively, the reduction of metal precursor also performed on a carbon nanotube surface electrochemically by allowing current through an aqueous metal salt solution with carbon nanotubes as one of the electrode.[21-22] In order to achieve noble metal nanoparticles decorated HNTs with enhanced properties, the rich coordination nature of metal ions along with multi-chelating ligands play a major role and provide versatility from both the structural as well as functional aspects.[23] In order to mimic nanotubular structure, the molecular structure of the complexes utilized during the synthetic process dictates the structure and shape of resulting hybrid nanomaterials.[24]

Decomposing metal salts thermally (i.e., pyrolysis) have been followed repeatedly for the preparation of metal-containing nanoparticles and nanorods.[25-27] Of course, to achieve nanometer scaled particles, the metal precursor decomposition normally performed at a slower heating rate and/or in a solvent medium.[28] Studies on the direct metal precursor decomposition in the presence of nanosized substrates[29-31] including carbon nanotubes[32-35] for the preparation of nanohybrid materials have been quite less explored. In Chen et al. report, aluminium oxide with an inner pore diameter of 0.05 μm and height of 60 μm were utilized as a template for the preparation of Ru-Pt-core/Nafion-sheath composite nanotubes by a dip-and-dry process.[36] Park et al. reported silver nanoparticles (Ag NPs) decorated poly(3,4-ethylenedioxythiophene) (PEDOT) nanotubes via vapour deposition polymerization (VDP) methodology.[37]

We have been working on design, synthesis and characterization of functionalized monolayer materials.[38-42] In the present study,

we synthesized Ag NPs decorated hybrid nanotubes (HNTs) as one-dimensional inorganic hybrids by simply refluxing Ag nitrate with Ru(II)-sensitizer. Here, Ag NPs used as building blocks and Ru(II)-sensitizer as three-dimensionally connecting molecular unit to form various Ru(II)-Ag hybrid nanostructures. HNTs formation process performed by excluding structure directing templates like nanoporous alumina[43] or carbon nanotube with anionic functionalities.[44] Compared to most of the synthetic strategies adopted so far,[45] this is simple method involving, "mix-and-reflux" in the presence of mixture of solvents. In addition, this study covers the effect of Ag nitrate concentration over molecular-assembly, Ag loading levels in hybrid nanostructures, role of capping agents used, optical properties performed and evaluated to interpret the synthetic mechanism.

2. Materials and methods

4,4'-Dimethyl-2,2'-bipyridine (99.5%), and $RuCl_3.3H_2O$ were purchased from Sigma-Aldrich. $AgNO_3$ (99+%) and trisodium citrate dihydrate (99%) were purchased from Alfa Aesar, Massachusetts, USA. Acetonitrile (HPLC grade) was purchased from Rankem, India, while absolute ethanol (99.9%) was received from J. H. Inter. trade co. Ltd, China. All chemicals of highest purity were used as such. All aqueous solutions were prepared using double distilled water unless otherwise specified. All glasswares treated with acid and cleaned with ample amount of double distilled water prior to use.

2.1 Measurements

The morphologies of materials analysed and its elemental composition performed using transmission electron microscopy (TECNAI G^2 T30) working at 300 kV accelerating voltage coupled with EDS facility. Additionally, scanning electron microscopy (SEM) images captured using EVO/ MA 15 ZEISS instrument operating at 20.0 kV accelerating voltage. In the sample preparation, nanomaterials diluted in ethanol were cast onto a copper grid/microscopic cover glass for electron microscopic studies. The powder X-ray diffraction pattern was recorded using Rigaku Miniflex diffractometer employing Cu-K(α) radiation. The electronic absorption spectra were recorded using a Jasco V-670 spectrophotometer at room temperature. The electronic emission spectra were recorded on a Varian Cary Eclipse Fluorescence Spectrophotometer at room temperature. The Raman spectra of Ag nanocomposite particles and HNTs on microscopic cover glass were recorded using a Renishaw invia Raman spectrometer using laser of 785 nm from HPNIR diode laser source. In all Raman spectra measurements, spectral resolutions (with a grating of 1200 lines/mm) of 1 cm^{-1} have been achieved. The signals were collected (10 s) in a backscattering geometry and guided to an air-cooled charge-coupled device (CCD) detector. The Ru(II)-Ag nanostructures with various ratios were separated by centrifugation and washed repeatedly with the solvent mixture (ACN: EtOH: H_2O, 3:1:1 v/v). The resulting material dispersed in 5 ml solvent mixture for optical studies.

2.2 Sample preparation for Raman scattering studies

About 1 ml of Ru(II)-Ag nanostructure solutions were dropped on cleaned microscopic cover glass and allowed to dry at room temperature in dark. Thus obtained dry thin films utilized to characterize SERS performance of Ru(II)-Ag NCs and HNTs.

2.3 Fluorescence spectroscopy sample preparation

In each case, 250 µl of Ru(II)-Ag nanostructure solutions were dispersed in 10 ml of the solvent mixture (ACN: EtOH: H_2O, 3:1:1 v/v) and fluorescence performance were measured by exciting the sample at 460 nm.

2.4 UV-Vis spectroscopy

The electronic absorption spectra of Ru(II)-Ag nanostructures obtained by dispersing 250 µl of each sample in 3ml of the solvent mixture (ACN: EtOH: H_2O, 3:1:1 v/v) and recorded in the range of 200-800 nm.

2.5 Preparation of citrate stabilized Ag NPs

Literature procedure followed for the synthesis of colloidal citrate stabilized Ag NPs as mentioned in previous work.[46]

2.6 Preparation of Ag NPs decorated hybrid nanotubes (HNTs)

4,4'-Dicarboxy-2,2'-bipyridine, $Ru(H_2dcbpy)_3].6H_2O$ were prepared following literature procedure.[47,48] Briefly, $[Ru(H_2dcbpy)_2(dcbpy)].6H_2O$ (96 µmol) was mixed with $AgNO_3$ (using concentration from 0.1 to 0.6 mmol) in 10 ml of ACN:EtOH:H_2O (3:1:1 v/v). The resulting mixture was sonicated, followed by reflux over oil bath at 80°C for 24hr in dark under nitrogen atmosphere. This procedure was followed for all set of reactions throughout the synthesis of hybrid nanostructures.

3. Results and discussion

The molecular structures employed to syntheses of Ag nanostructures are, tris(4,4'-dicarboxy-2,2'-bipyridine) ruthenium(II)hexahydrate, trisodium citrate dihydrate molecules.

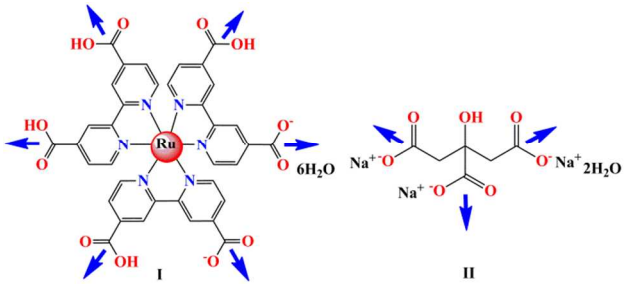

Fig. 1. The molecular structure of capping agents used in the present study are, (I) tris(4,4'-dicarboxy 2,2'-bipyridine)ruthenium(II)hexahydrate, (II) trisodium citrate dihydrate.

Among these two molecules, the structural difference is that, molecular rigidity with aromatic rings in Ru(II)-sensitizer with six carboxylate (-COOH) groups (I) and structural flexibility in trisodium citrate molecule with three -COOH groups (II). This contrast structural feature in two molecules play a vital role in forming Ru(II)-Ag hybrid nanostructures and citrate capped few Ag nanorod with spherical nanoparticles.

The reducing and stabilizing chemistry of -COOH group over Ag precursor is well established in many reports.[49] By taking the advantage of rich coordination carboxylate chemistry, 2,2'-bipyridine ligand functionalized with -COOH group at 4,4'-position known for three dimensional binding ability and by incorporating Ru(II)-metal through N-atoms which control number of coordination sites toward Ag^+ ion and enhance Ag^+ ion reducing ability and thus act as a structure directing molecular linker for Ag NPs.[50]

The formation of Ag NPs and hybrid nanostructures in the presence of mixture of solvents (ACN: EtOH: H_2O) are represented in Figure 2.

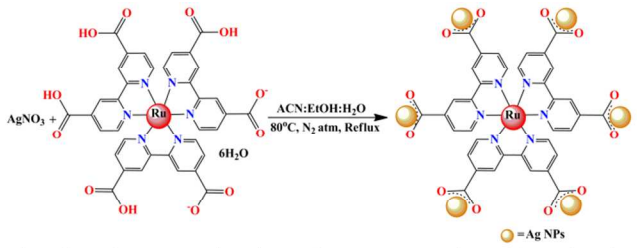

Fig. 2. The general schematic representation of molecular-assembly in presence of Ag NPs with tris(4,4`-dicarboxy-2,2`-bipyridyl)ruthenium(II).

Electron microscopy (TEM, SEM) studies clearly suggested the progressive formation of hybrid nanostructures starting from Ag NPs and also partially underwent misfolded irregular sheets for $[Ag^{+}/Ru^{2+}]$ ratio = 1.04 (Figure 3A and Figure S1). The irregular sheet became open ended regular tube shape with well-defined morphologies for $[Ag^{+}/Ru^{2+}]$ ratio = 3.1 shown in Figure 3B.

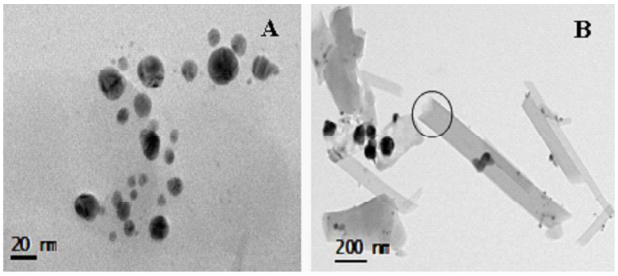

Fig. 3. (A) Representative TEM micrograph of Ru(II)-Ag nanoparticles with $[Ag^{+}/Ru^{2+}]$ ratio = 1.04. (B) TEM micrograph represents HNTs with broken open ended morphology having diameter greater than 100 nm with $[Ag^{+}/Ru^{2+}]$ ratio = 3.1.

The diameter of HNTs is formed in the range of > 2 µm length, 90-110 nm wider with $[Ag^{+}/Ru^{2+}]$ = 4.2 as given in Figure S3 and Figure 4. In this reaction conditions, Ru(II)-sensitizer and Ag NPs are well assembled to form longer range HNTs with 4 ± 2 nm sized Ag NPs. Additionally, hetero droplet Ag NPs 50 ± 5 nm in size observed and submerged on hybrid nanotube wall. Such a large diameter nanotubes might be attractive for catalysis and nanoelectronic circuit connectors.[51]

To analyse structural chemical components of hybrid nanostructures, nanoprobe X-ray energy dispersive spectrometry (EDS) and selected area electron diffraction (SAED) studies were performed which showed that, all hybrid nanostructures were decorated with crystalline Ag NPs and were composed of Ru(II)-sensitizer and Ag^{0} NPs (Figure S4- S7 and table S2). Moreover, the presence of single peak at 38° with (111) crystal plane further confirmed Ag NPs crystallinity on hybrid nanostructures as shown by powder X-ray diffraction (PXRD) profile (Figure S9). No peaks were seen at 44.2°, 64.3°, 77.2° for Ag^{0} crystal planes (200), (220), (311) strongly suggest that Ag NPs are crystalline with (111) plane.[52]

By increasing $[Ag^{+}/Ru^{2+}]$ ratio from 4.2 to 5.2, IINTs change from open ended to closed tube morphology with hetero droplet Ag NPs at their outer surface which had length of 800 ± 10 nm and width of 100 ± 10 nm (Figure 5). In $[Ag^{+}/Ru^{2+}]$ ratio = 6.4, similar effects are observed with increase in size and intensity of hetero droplet Ag NPs over walls of HNTs (Figure 6). Ag NPs loaded over HNTs are 15 ± 5 nm in size and HNTs having 470 ± 10 nm in length, 95 ± 5 nm in diameter.

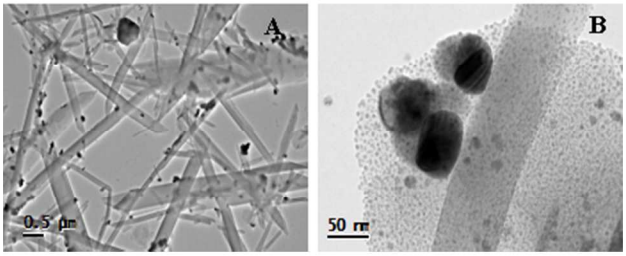

Fig. 4. (A) TEM micrograph represents the formation of long range HNTs having length of greater than 2 µm. (B) A close view of hetero droplet Ag^{0} NPs in contact with the hybrid nanotube surface.

Additionally, hetero droplet Ag NPs population high than Ag^{+}/Ru^{2+} ratio 5.2, informs that the saturation level of Ag NPs in molecular-assembly process and deposition over HNT walls. The transition from Ag NCs to HNTs formation clearly evidenced by analysing SEM micrograph for ratio Ag^{+}/Ru^{2+} = 2.0, where HNTs cum sheets are formed as a major product (Figure S8).

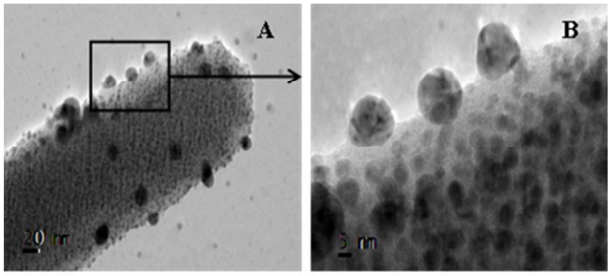

Fig. 5. (A) Representative TEM micrographs of hybrids surface composed with Ag NPs obtained with $[Ag^{+}/Ru^{2+}]$ = 5.2. (B) A close look of Ag NPs having size of 10 ± 2 nm on HNT.

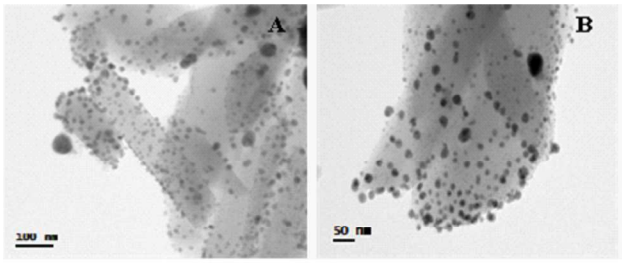

Fig. 6. (A) Representative TEM micrographs of hybrid nanotubes surface composed with Ag NPs obtained with $[Ag^{+}/Ru^{2+}]$ = 6.4. (B) A close look of Ag NPs having size of 15±5 nm on hybrid nanostructures.

The evolution of carbon and inorganic nanotubular morphologies involve the assembly of many number of sheets followed by a folding process.[53] In an initial reaction condition, misfolded sheets with Ag NPs having irregular morphology were observed which was not suitable to form HNTs (Figure S1). No HNTs and sheets were observed when the reaction was performed at room temperature by only sonication for longer period of time. But, by applying heat, sub-10 nm Ag NPs were observed on the walls of thus formed HNTs, and were achieved with longer length-to-diameter ratio. These observation suggest that the optimal level of Ag nitrate with suitable Ru(II)-sensitizer concentration in the reaction mixture is essential to achieve uniform Ag NPs loading as well as length of HNTs through self-assembly process.

3.1 Effect of capping molecules

In presented work, the different nanostructures were noticed at

distinct applied reaction ratios. Hetero droplet Ag^0 NPs on HNTs were noticed at higher ratio of two components [Ag^+/Ru^{2+}] = 4.2, whereas for lower ratio of the same components [Ag^+/Ru^{2+}] = 1.04, decahedron (Dh) Ag nanocomposites were observed which are shown in Figure 4B-6B and 7A respectively. These structural features are assigned by analysing reports for Ag nanostructures.[54] First, decahedron (Dh) shape formation were considered as the assembly of five Ag^0 single crystal tetrahedral units sharing a common edge, which comes into contact with neighbour units through (111) plane and the defected part keep increase in area as decahedral seed form and then enlarge laterally. At final stage, multiply twinned seeds were only preferred thermodynamically at small sizes.[55] The study report on Ag NPs by Ferrando et al., informed that, icosahedron shaped particles were found to be stable at relatively small sizes, decahedron shaped particles at medium sizes for fcc metal.[56] From this comparative studies, we concluded that the presence of -COOH groups over Ru(II)-sensitizer and applied reaction conditions favoured thermodynamically stabilizing (111) crystal plane and lead to decahedron (Dh) shaped Ag NCs formation as a product (Figure 7A).

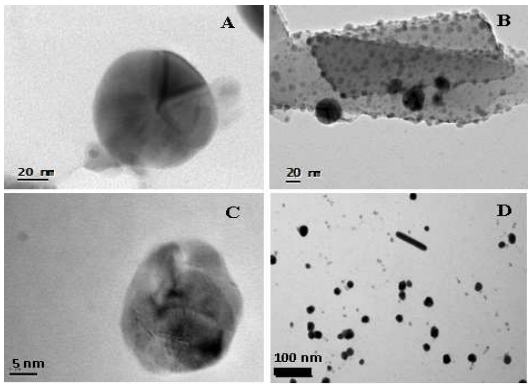

Fig. 7. (A) Representative TEM micrographs obtained with Ru(II)-Ag decahedron nanocomposite particles observed with [Ag^+/Ru^{2+}]= 1.04. (B) Ru(II)-Ag HNTs obtained with length-to-diameter (> 100 nm in diameter) obtained with molar ratio of [Ag^+/Ru^{2+}] = 4.2. (C) Citrate capped Ag NPs with twinned decahedron (Dh) shape. (D) Citrate capped Ag nanorod of about 80 nm in length.

In order to see the effect of -COOH functionality in the Ag nanostructures formation, we selected two different molecules with same -COOH functional group. In case of ruthenium functionalized Ag NCs, it forms decahedron nanocomposites at lower ratio ([Ag^+/Ru^{2+}] = 1.04) while hybrid nanotubes were formed with increasing concentration of Ag nitrate. Further, similar –COOH functionality, in case of citrate capped Ag NPs, a nanorod structure was observed along with Ag twinned decahedron (Dh) nanoparticles suggested that, a capping molecule with more than one -COOH group might be able to produce nanorod, but in case of aromatic -COOH groups on Ru(II)-sensitizer produce nanotubular morphology (Figure 7B-D) rather than nanorod morphology.

3.2 Optical studies of Ru(II)-Ag hybrid nanostructures

The electronic absorption spectra of resulting Ru(II)-Ag nanostructures were confirmed the formation of Ag NPs loaded HNTs. The surface plasmon of Ag NPs observed at 426 nm[49] and MLCT of Ru(II)-sensitizer at 480 nm.[48]

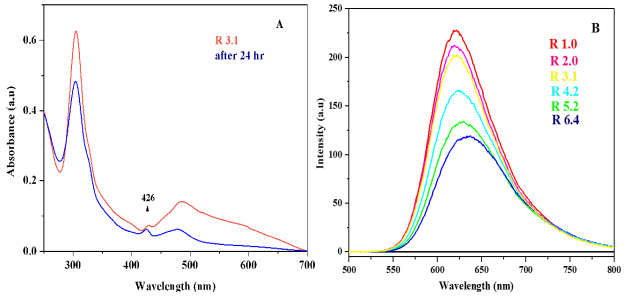

Fig. 8. (A) The electronic absorption spectra of Ru(II)-Ag hybrid nanostructure with [Ag^+/Ru^{2+}] = 3.1, showed plasmon band of Ag NPs at 426 nm along with MLCT band of Ru(II)-sensitizer at 480 nm. (B) The emission spectra of Ru (II)-Ag hybrid nanostructures recorded by exciting the samples at 460 nm, where R = Ratio.

The emission spectra showed that all Ru(II)-Ag hybrid nanostructures highly fluorescent active in the region of 620-635 nm (Figure 8B). Optically, citrate stabilized Ag NPs showed surface plasmon resonance band at 420 nm and its progressive Ag nanocluster growth monitored upto 48 days and showed red shift in UV-vis spectra shown in Figure S10.

3.3 Raman spectroscopy on Ag NPs decorated hybrid nanostructures

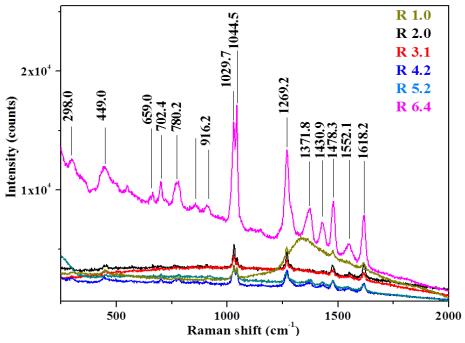

Fig. 9. The Raman scattering pattern of Ru(II)-Ag hybrid nanostructures at excitation of 785 nm, showing the scattering enhancement in Ag NPs decorated hybrid nanostructures, R = Ratio.

The optical Raman scattering properties of Ag nanostructures are well documented phenomena.[57] In order to evaluate optical properties of nanostructures formed in this study, we used 785 nm laser Raman excitation for scattering studies. The chemical proximity of the Ag NPs to the nanotubes is expected to induce the electronic transitions (charge transfer), which can be explored in Raman spectroscopy studies.[58] The surface enhancement results from the interaction of chemisorbed Ru(II)-sensitizer molecules with ballistic ("hot") electrons that are generated through plasmon excitation from Ag NPs surface and thus enhanced Raman signal[59] in hybrid nanostructures shown in Figure 9. Enhancement of Raman signals indicated that increase of Ag NPs load on HNTs enhances scattering property of hybrid nanostructures in the same order. This informed that nanohybrids with different composition and size of Ag NPs might be act as SERS probes for single molecule studies.

4. Conclusions

A novel one-pot method was reported for the preparation of Ag NPs decorated HNTs using Ag nitrate as metal precursor and

Ru(II)-sensitizer as molecular linker without the use of any commercial reducing agent or templates. The formation of Ag NPs and HNTs processes observed as a result of in situ coordination polymerization phenomena.

Thus obtained Ag NPs decorated hybrid nanostructures characterized in detail via various instrumental techniques such as TEM with EDS, SAED, SEM, PXRD, optical absorption and emission spectroscopy, Raman spectroscopy. The average nanoparticle size increased with high Ag nitrate concentration. The molar ratio $[Ag^{+}/Ru^{2+}]$ = 4.2 was proved to be excellent combination of molecules with Ag NPs as building units in order to achieve uniform Ag-loading in sub-10-nm size and long range HNTs. Raman studies showed that nanohybrids are suitable materials for optical scattering studies and single molecule probing processes. These Ru(II)-Ag hybrid plasmonic-nanostructures may act as promising materials for efficient heterogeneous photo-catalyst for energy conversion system[60] and in nanoelectronics fabrication.[61] These findings, in general, indicate that the molecules with well-designed architecture, combined with the bottom-up approach, can be effectively used to synthesis of Ag NCs to hybrid nanostructures of up to several micrometers long approaching > 2 μm. The various metals that can coordinate to the used molecule open up new avenue to form novel hybrid nanostructures with fascinating properties.

Acknowledgements

NV acknowledges financial support from DST Nanomission (SR/NM/NS-12/2010), Govt. of India, India and Dr N. C. Mehra, Department of Geology, University of Delhi, India for providing SEM facility. SKA thanks University of Delhi for in part financial support.

Notes and references

[a] *Chemical Biology Laboratory, Department of Chemistry, University of Delhi, Delhi-100 007, India. Tel: +91-9582087608; E-mail: skawasthi@chemistry.du.ac.in*

[b] *Faculty of Life Sciences and Biotechnology, South Asian University, New Delhi-110021, India. Tel: +919999074473; E-mail: rdgupta@sau.ac.in*

† Electronic Supplementary Information (ESI): [Fig. S1 TEM of Ru(II)-Ag I hybrid misfolded sheets. Fig. S2 TEM and electron diffraction (ED) of Ru(II)-Ag III hybrid nanotubes (HNTs). Fig. S3 TEM and ED of Ru(II)- Ag IV HNTs. Fig. S4 TEM and ED of Ru(II)- Ag V HNTs. Fig. S5 TEM and ED of Ru(II)-Ag VI wider HNTs. Fig. S6 TEM and ED of citrate-Ag NPs with nanorod. Fig. S7 EDS of Ru(II)-Ag hybrid nanostructures. Fig. S8 SEM of Ru(II)-Ag hybrids molar ratio = 2.0, 5.4. Fig. S9 PXRD pattern of Ru(II)-Ag HNTs. Fig. S10 UV-Vis spectra of citrate-Ag NPs. Table S1. Summary of experiment details and morphologies. Table S2. Summary of EDS analysis]. See DOI: 10.1039/b000000x/

1 (a) J. Hu, T. W. Odom and C. M. Lieber *Acc. Chem. Res.*1999, **32**, 435-445; (b) C. J. Murphy, A. M. Gole, S. E. Hunyadi and C. J. Orendorff *Inorg. Chem.* 2006, **45**, 7544-7554; (c) J. Goldberger, R. Fan and P. Yang *Acc. Chem. Res.* 2006, **39**, 239-248; (d) L. A-Abramovich, M. Reches, V. L. Sedman, S. Allen, S. J. B. Tendler and E. Gazit *Langmuir* 2006, **22**,1313-1320.

2 (a) A. B. Castle, E. G-Espino, C. N-Delgado, H. Terrones, M. Terrones and S. Hussain *ACS Nano* 2011, **5**, 2458-2466; (b) D. M. Kalaskar, C. Poleunis, C. D-Gillain and S. D-Champagne *Biomacromolecules* 2011, **12**, 4104-4111; (c) S. H. Han and J-S. Lee *Langmuir* 2012, **28**, 828-832; (d) E. Katz and I. Willner *ChemPhysChem* 2004, **5**, 1084-1104.

3 (a) A. Dorn, D. B. Strasfeld, D. K. Harris, H-S. Han and M. G. Bawendi *ACS Nano* 2011, **5**, 9028-9033; (b) S. De, T. M. Higgins, P. E. Lyons, E. M. Doherty, P. N. Nirmalraj, W. J. Blau, J. J. Boland and J. N. Coleman *ACS Nano* 2009, **7**, 1767-1774; (c) Y. Li, C. Li, S. O. Cho , G. Duan and W. Cai *Langmuir* 2007, **23**, 9802-9807; (d) G. Che, B. B. Lakshmi, E. R. Fisher and C. R. Martin *Nature* 1998, **393**, 346-349; (e) E. S. Steigerwalt, G. A. Deluga and C. M. Lukehart *J. Phys. Chem. B* 2002, **106**, 760-766.

4 (a) M. Feng, M. Zhang, J-M. Song, X-G. Li and S-H. Yu *ACS Nano* 2011, **5**, 6726-6735; (b) L. N. Lewis *Chem. Rev.*1993, **93**, 2693-2730.

5 (a) H. Jia, X. Bai, N. Li, L. Yua and L. Zheng *CrystEngComm* 2011, **13**, 6179; (c) N. Ravichandra raju and K. J. Kumar *J. Raman Spectrosc.* 2011, **42**, 1505-1509; (d) X. S. Shen, G. Z. Wang, X. Hong and W. Zhu *Phys. Chem. Chem. Phys.* 2009, **11**, 7450-7454; (e) L-M. Chen and Y-N. Liu *CrystEngComm* 2011, **13**, 6481.

6 (a) C. N. R. Rao and A. Govindaraj *Adv. Mater.* 2009, **21**, 4208-4233; (b) W. Zhou, X. Bai, E. Wang and S. Xie *Adv. Mater.* 2009, **21**, 4565-4583; (c) M. A. Correa-Duarte and L. M. Liz-Marzan *J. Mater. Chem.* 2006, **16**, 22-25; (d) Y. Saito, K. Nishikubo, K. Kawabata and T. Matsumoto *J. Appl. Phys.*1996, **80**, 3062-3067.

7 (a) G. G. Wildgoose, C. E. Banks and R. G. Compton *Small* 2006, **2**, 182-193; (b) P. C. Hidber, W. Helbig, E. Kim and G. M. Whitesides *Langmuir* 1996, **12**, 1375-1380.

8 V. Georgakilas, D. Gournis, V. Tzitzios, L. Pasquato, D. M. Guldi and M. Prato *J. Mater. Chem.* 2007, **17**, 2679-2694.

9 Y. Xia, P. Yang, Y. Sun, Y. Wu, B. Mayers, B. Gates, Y. Yin, F. Kim and H. Yan *Adv. Mater.* 2003, **15**, 353-389.

10 A. N. Shipway, E. Katz and I. Willner *ChemPhysChem* 2000, **1**, 18-52

11 (a) G. Shen, Y. Bando and D. Golberg *J. Phys. Chem. B* 2006, **110**, 23170-23174; (b) R. Ma, T. Sasaki and Y. Bando *J. Am. Chem. Soc.* 2004, **126**, 10382-10388.

12 J. Couet, J. D. J. S. Samuel, A. Kopyshev, S. Santer and M. Biesalski *Angew. Chem. Int. Ed.* 2005, **44**, 3297-3301.

13 C. A. Mirkin, R. L. Letsinger, R. C. Mucic and J. J. Storhoff *Nature* 1996, **382**, 607-609.

14 R. Djalali,Y. Chen and H. Matsui *J. Am. Chem. Soc.* 2002, **124**, 13660-13661.

15 R. G. Freeman, K. C. Grabar, K. J. Allison, R. M. Bright, J. A. Davis, A. P. Guthrie, M. B. Hommer, M. A. Jackson, P. C. Smith, D. G. Walter and M. J. Natan *Science* 1995, **267**, 1629.

16 (a) E. Abdullayev, K. Sakakibara, K. Okamoto, W. Wei, K. Ariga and Y. Lvov *ACS Appl. Mater. Interfaces* 2011, **3**, 4040-4046; (b) M. Wirtz, M. Parker,Y. Kobayashi and C. R. Martin *Chem. Eur. J.* 2002, **8**, 3572-3578; (c) J. Sloan, D. M. Wright, H-G. Woo, S. Bailey, G. Brown, A. P. E. York, K. S. Coleman, J. L. Hutchison and M. L. H. Green *Chem. Commun.*1999, **8**, 699-700; (d) S-H. Zhang, Z-X. Xie, Z-Y. Jiang, X. Xu, J. Xiang, R-B. Huang and L-S. Zheng *Chem. Comm.* 2004, **9**, 1106-1107; (e) C. Bae, H. Yoo, S. Kim, K. Lee, J. Kim, M. M. Sung and H. Shin *Chem. Mater.* 2008, **20**, 756-767; (f) R-X. Dong, W-C. Tsai and J-J. Lin *Eur. Polym. J.* 2011, **47**, 1383-1389.

17 M. Lahav, T. Sehayek, A. Vaskevich and I. Rubinstein *Angew. Chem. Int. Ed.* 2003, **42**, 5576-5579.

18 J. M. Planeix, N. Coustel, J. Coq, V. Brotons, P. S. Kumbhar, R. Dutartre, P. Geneste, P. Bernier and P. M. Ajayan *J. Am. Chem. Soc.*1994, **116**, 7935-7936.

19 B. Xue, P. Chen, Q. Hong, J. Lin and K. L. Tan *J. Mater. Chem.* 2001, **11**, 2378-2381.

20 V. Lordi, N. Yao and J. Wei *J. Chem. Mater.* 2001, **13**, 733-737.

21 B. M. Quinn, C. Dekker and S. G. Lemay *J. Am.Chem. Soc.* 2005, **127**, 6146-6147.

22 T. M. Day, P. R. Unwin, N. R. Wilson and J. V. Macpherson *J. Am. Chem. Soc.* 2005, **127**, 10639-10647.

23 (a) R. Kaminker, R. Popovitz-Biro and M. E. van der Boom *Angew. Chem. Int. Ed.* 2011, **50**, 3224-3226; (b) F. Wang, J. Zahng, X. Ding, S. Dong, M. Liu, B. Zheng, S. Li, L. Wu, Y. Yu, H. W. Gibson and F. Huang *Angew. Chem. Int. Ed.* 2010, **49**, 1090-1094.

24 (a) B. W. Jacobs, R. J. T. Houk, M. R. Anstey, S. D. House, I. M. Robertson, A. A. Talinc and M. D. Allendorf *Chem. Sci.* 2011, **2**, 411-416; (b) T. Tsuruoka, H. Kawasaki, H. Nawafune and K. Akamatsu *ACS Appl. Mater. Interfaces* 2011, **3**, 3788-3791; (c) A. Umemura, S. Diring, S. Furukawa, H. Uehara, T. Tsuruoka and S. Kitagawa *J. Am. Chem. Soc.* 2011, **133**, 15506-15513.

25 (a) Y. Wang and Y. Xia *Nano Lett.* 2004, **4**, 2047-2050; (b) A. Govindaraj, S. R. C. Vivekchand and C. N. R. Rao *J. Nanosci. Nanotechnol.* 2007, **7**, 1695; (b) H. Guan, C. Shao, S. Wen, B. Chen, J. Gong and X. Yang *Inorg. Chem. Commun.* 2003, **6**, 1302-1303.

26 (a) F. X. Redl, C. T. Black, G. C. Papaefthymiou, R. L. Sandstrom, M. Yin, H. Zeng, C. B. Murray and S. P. O'Brien *J. Am. Chem. Soc.* 2004, **126**, 14583-14599.

27 R-Q. Song, A-W. Xu, B. Deng, Q. Li and G. Y. Chen *Adv. Funct. Mat.* 2007, **17**, 296-306.

28 C. Burda, X. Chen, R. Narayanan and M. A. El-Sayed *Chem. Rev.* 2005, **105**, 1025-1102.

29 L.Vovchenko, L. Matzui, M. Zakharenko, M. Babich and A. Brusilovetz *J. Phys. Chem. Solids* 2004, **65**, 171-175.

30 J. Miyawaki, M. Yudasaka, H. Imai, H. Yorimitsu, H. Isobe, E. Nakamura and S. Iijima *Adv. Mater.* 2006, **18**, 1010-1014.

31 Y. Li, E. J. Lee and S. O. Cho *J. Phys. Chem. C* 2007, **111**, 14813-14817.

32 Y-L. Yao, Y. Ding, L-S. Ye and X-H. Xia *Carbon* 2006, **44**, 61-66.

33 Y-J. Gu and W-T. Wong *Langmuir* 2006, **22**, 11447-11452.

34 K-F. Yung and W-T. Wong *J. Cluster Sci.* 2007, **18**, 51-65.

35 N. Karousis, G-E. Tsotsou, F. Evangelista, P. Rudolf, N. Ragoussis and N. Tagmatarchis *J. Phys. Chem. C* 2008, **112**, 13463-13469.

36 J. Chen, Z-L. Tao and S-L. Li *J. Am. Chem. Soc.* 2004, **126**, 3060-3061.

37 E. Park, O. Kwon, S. Park, J. Lee, S. You and J. Jang *J. Mater. Chem.* 2012, **22**, 1521-1526.

38 T. Gupta, P. C. Mondal, A. Kumar, Y. L. Jeyachandran and M. Zharnikov *Adv. Funct. Mater.* 2013, **23**, 4227-4235.

39 P. C. Mondal, Y. L. Jeyachandran, H. Hamoudi, M. Zharnikov and T. Gupta *J. Phys. Chem. C* 2011, **115**, 16398-16404.

40 N. Vilvamani, S. Deka and T. Gupta *Adv. Mater. Lett.* 2013, **4**, 52-60.

41 D. A. Cristaldi, A. Motta, S. Millesi, T. Gupta, M. Chhatwal and A. Gulino *J. Mater. Chem. C* 2013, **1**, 4979-4984.

42 V. Singh, P.C. Mondal, Y. L. Jeyachandran, M. Zharnikov and T. Gupta *Analyst* 2012, **137**, 3181-3192.

43 L. Qu, G. Shi, X. Wu and B. Fan *Adv. Mater.* 2004, **16**, 1200-1203.

44 P. Diao and Z. Liu *Adv. Mater.* 2010, **22**, 1430-1449.

45 Y. Lin, K. A. Watson, M. J. Fallbach, S. Ghose, J. G. Smith, J. D. M. Delozier, W. Cao, R. E. Crooks and J. W. Connell *ACS Nano* 2009, **3**, 871-884.

46 J. Turkevich, R. C. Stevenson and J. Hillier *J. Phys. Chem.* 1953, **57,** 670-673.

47 S. Fuldner, R. Mild, H. I. Siegmund, J. A. Schroeder, M. Gruber and B. Konig *Green Chem.* 2010, **12**, 400-406.

48 E. Eskelinen, S. Luukkanen, M. Haukka, M. Ahlgren and T. A. Pakkanen *J. Chem. Soc. Dalton Trans.* 2000, **16**, 2745-2752.

49 M. Yamamoto, Y. Kashiwagi and M. Nakamoto *Langmuir* 2006, **22**, 8581-8586.

50 Y-H. Liu, Y-L. Lu, H-C. Wu, J-C. Wang and K-L. Lu *Inorg. Chem.* 2002, **41**, 2592-2597.

51 (a) M. Koshino, Y. Niimi, E. Nakamura, H. Kataura, T. Okazaki, K. Suenaga and S. Iijima *Nat. Chem.* 2010, **2**, 117-124; (b) M. Remskar, A. Mrzel, M. Virsek and A. Jesih *Adv. Mater.* 2007, **19**, 4276-4278.

52 Y. Sun, Y. Yin, B. T. Mayers, T. Herricks and Y. Xia *Chem. Mater* 2002, **14**, 4736-4745.

53 (a) S. Iijima *Nature* 1991, **354**, 56-58; (b) W. Tremel *Angew. Chem. Int. Ed.*1999, **38**, 2175-2179.

54 (a) Y. Xia, Y. Xiong, B. Lim and S. E. Skrabalak *Angew. Chem. Int. Ed.* 2009, **48**, 60-103; (b) D. J. Smith, A. K. Petford-Long, L. R. Wallenberg and J. O. Bovin *Science* 1986, **233**, 872; (c) S. Iijima and T. Ichihashi *Phys. Rev. Lett.*1986, **56**, 616-619; (d) N. Doraiswamy and L. D. Marks *Surf. Sci.*1996, **348**, 67-69; (e) H. B. Liu, J. A. Ascencio, M. Perez-Alvarez and M. J. Yacaman *Surf. Sci.* 2001, **491**, 88-98.

55 (a) P. L. Gai and M. A. Harmer *Nano Lett.* 2002, **2**, 771-774; (b) C. Lofton and W. Sigmund *Adv. Funct. Mater.* 2005, **15**, 1197-1208; (c) J. L. Elechiguerra, J. Reyes-Gasga and M. J. Yacaman *J. Mater. Chem.* 2006, **16**, 3906-3919.

56 (a) F. Baletto and R. Ferrando *Phys. Rev. B* 2001, **63**, 155408-155410; (b) F. Baletto, R. Ferrando, A. Fortunelli, F. Montalenti and C. Mottet *J. Chem. Phys.* 2002, **116**, 3856-3863; (c) F. Baletto and R. Ferrando *Rev. Mod. Phys.* 2005, **77**, 371-423.

57 A. Otto, I. Mrozak, H. Grabhorn and W. Akemann *J. Phys. Condens. Matter* 1992, **4**, 1143-1212.

58 A. M. Michaels, M. Nirmal and L. E. Brus *J. Am. Chem. Soc.*1999 **121**, 9932-9939.

59 B. N. J. Persson *Chem. Phys. Lett.*1981, **82**, 561-565.

60 S. Linic, P. Christopher and D. B. Ingram *Nature Mater.* 2011, **10**, 911-921.

61 J. Zhao, H. Sun, S. Dai, Y.Wang and J. Zhu *Nano Lett.* 2011, **11**, 4647-4651.

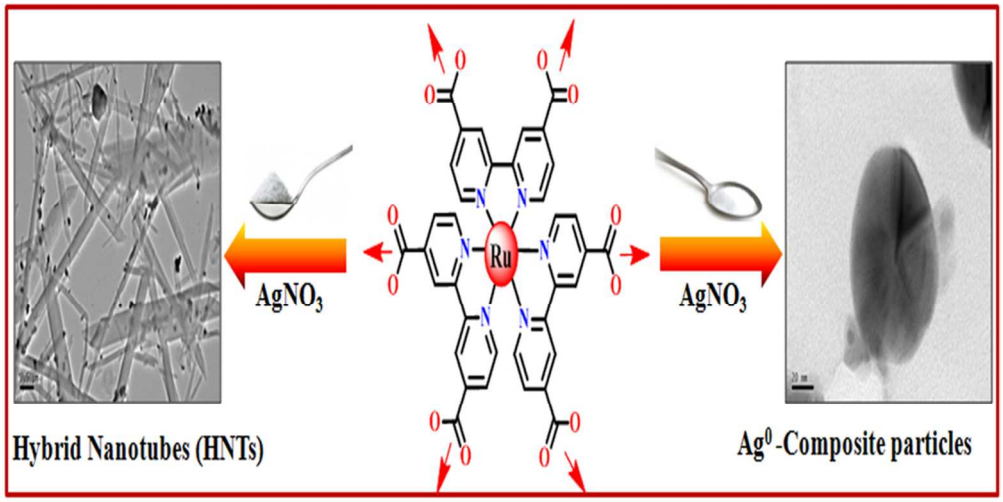

Facile and templateless one-pot synthesis of Ru(II)polypyridyl complex-based hybrid nanostructures decorated with silver nanoparticles (Ag NPs) with variable morphologies
40x20mm (600 x 600 DPI)